POAC'17
Busan, KOREA

Proceedings of the 24th International Conference on
Port and Ocean Engineering under Arctic Conditions
June 11-16, 2017, Busan, Korea

2D Numerical Modeling of Icebreaker Advancing in Ice-covered Water

Junji Sawamura[1]
[1] Department of Naval Architecture and Ocean Engineering Osaka University, Osaka, Japan

ABSTRACT

This paper presents a 2D numerical modeling to calculate removal and breaking of ice floes when an icebreaker advances into ice-covered water. The numerical simulation calculates repeatable ice-breaking and ice-removal in pack ice. The ice-breaking is calculated by a ship-ice contact detection and fluid-structural interaction of bending behavior of a plate ice. The ice-removal are calculated by a physically based modeling using 3DOF rigid body equations. A ship advances with a constant speed or constant thrust. A plate ice is broken by bending and splitting mode. The ice foes drift with constant force in which ice floes are assumed to be drifting by wind and current. An open channel caused by the ice-breaking and ice-removal by icebreaker are numerically obtained. A simulated ice channel after icebreaker's advancing into ice-covered water depends on the floe size as well as the ship's rigid motion and ice drifting force. The numerical results show the proposed numerical model can be useful in order to identify an efficient way of ship handling in ice-covered water.

KEY WORDS: Ice management; Pack ice; Icebreaking; Numerical simulation

INTROCUDTION

Ice management using an icebreaker is vital for safe and efficient operations for vessels and offshore structures in ice-covered waters. During an ice management operations, an icebreaker opens a cannel behind her by removing and breaking of ice floes. An escorted vessel can reduces the ice load in the managed ice channels. For successful ice management operations, the estimation of the managed ice channels opened by an icebreaker, and planning of the management vessels and fleet deployment configuration are needed.

Hamilton et al. (2011) developed a numerical simulator and quantified the ice management performance using real ice conditions data. They numerically study the effects of the ice management strategies such as the number of icebreaker and icebreaker speed performance on the ice floe size in the managed ice channel. Farid et al. (2014) investigated the sea ice breaking pattern of several short-term ice management activities during the research cruise (OATRC, 2013), and proposed a preliminary analysis. The maximum floe size resulting from the numerical simulations was fairly equivalent to that of real ship trial. Lu et al. (2015, 2016) investigated fracturing phenomena of ice floe during icebreaker's ice management. They

proposed the theoretical models of in-plane and out-plan ice failure for implementing into the numerical simulator of ship-ice interaction (e.g., Lubbad and Løset, 2011). The numerical simulation, as shown above, has the potential to evaluate of ice management strategy efficiently.

This paper develops a 2D numerical modeling to calculate removal and breaking of ice floes when an icebreaker advances into ice-covered water. The numerical model can predict repetitive ice floe removal and plate ice breaking by icebreaker. The motion of ice floes and icebreaker are described by 3DOF rigid body equations. The ice floes is drifting with constant drifting force which assumed to be ice floe's drifting by wind or current. Example results show the distributions of the ice channels and time history of ice force in different ice conditions. The effect of ice drifting and ice floe size on the ice channel made by an icebreaker are investigated.

NUMERICAL MODELING

Interaction between Ship and Plate Ice

The numerical simulation of ship advancing into level ice has been developed by Sawamura et al. (2009). In the relative large ice floe, a ship repetitively contacts with the ice edge and breaks the plate ice in various ice failure mode such as bending, crushing and splitting. The repetitive ship–ice contacts are represented using circle contact detection (e.g. Dimgliana et al., 2000). Figure 1 shows a schematic whereby circle contact detection is applied to ship–ice contacts. A plate ice and ship waterline are represented by contact circles. When the ship waterline contacts with the ice edge, the distance of both contact circles between the ship and ice becomes zero. When the plate ice is broken, contact circles within the ice cusp are removed from the plate ice. Contact detection and removal of contact circles within the broken cusp are progressing as the ship advances. The circle contact detection allows us to detect the contact points between the two complicated objects in less computational time. The accuracy of ship–ice contact and icebreaking depends on the contact circle radius.

The ice edge at the ship–ice contact is crushed as a ship advancing distance. The ice force increases proportionally with increased crushing area of the ice edge. When an ice pressure on the crushing area is assumed to be a constant, the ice force induced by a ship–ice contact is given as:

$$F_{\mathrm{n}} = A_{\mathrm{c}}\sigma_{\mathrm{c}} \tag{1}$$

where A_{c} represents the crushing area induced by ship–ice contact. σ_{c} is the compressive strength of ice. F_{n} acts in the direction normal to the ice crushing surface. Crushing area A_{c} increases with the icebreaker's advancing distance into ice edge. As the deflection of the plate ice is assume to be neglected and the geometrical relation between ship and ice are considered (Figure 2), the contact area A_{c} is given as:

$$A_{\mathrm{c}} = \frac{1}{2\sin\theta_{\mathrm{s}}}\left(\tan\theta_{\mathrm{wf}} + \tan\theta_{\mathrm{wb}}\right)\cdot(vt\cos\theta_{\mathrm{c}})^2, \qquad 0 < t < \frac{h_{\mathrm{i}}\tan\theta_{\mathrm{s}}}{v\cos\theta_{\mathrm{c}}}$$

$$= \frac{1}{2\cos\theta_{\mathrm{s}}}\left(\tan\theta_{\mathrm{wf}} + \tan\theta_{\mathrm{wb}}\right)\cdot(2vth_i\cos\theta_{\mathrm{c}} - {h_i}^2\tan\theta_{\mathrm{s}}), \qquad t > \frac{h_{\mathrm{i}}\tan\theta_{\mathrm{s}}}{v\cos\theta_{\mathrm{c}}} \tag{2}$$

where v denotes the ship velocity, t is the ship advancing time into the ice edge, h_{i} is the ice

thickness, θ_c and θ_s are, respectively, the ship's entrance angle and the ship hull's inclined angle. θ_{wf} and θ_{wb} are the forward and backward edge angles at the contact point.

Kinematic friction takes into account in direction horizontal to the surface of ice crushing. Coulomb type friction is represented as:

$$F_f = \mu F_n \tag{3}$$

where μ denotes the friction coefficient between the ship and ice. A direction of frictional force is opposite to the relative velocity between ship and ice. The total ice force attributable to ship–ice interaction is related to ice breaking of a plate ice that is calculated by the sum of collision force F_n and friction force F_f.

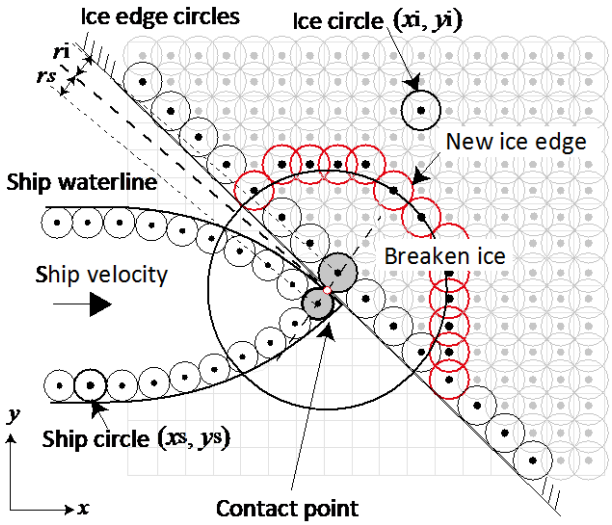

Figure 1. Circle contact detection applied to ship–ice interactions.

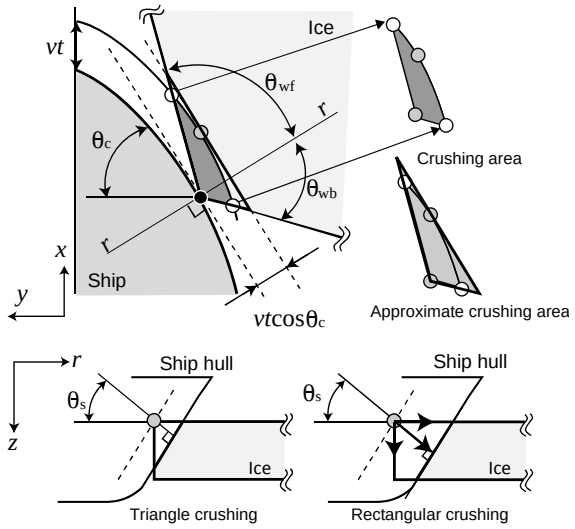

Figure 2. Ship-ice relation of ship-ice contact, ice crushing and ice contact force.

Plate Ice Breaking

A bending failure of plate ice occurs when the bending stress in the plate ice σ_b increases as the ship advances and exceeds the flexural strength of the ice, σ_f. The bending stress in the plate ice σ_b is calculated using a fluid–structure interaction (FSI) in which the dynamic effect of fluid underneath the plate ice is calculated as well as a plate ice bending (Sawamura et al., 2008). After bending failure, a circler ice cusp is broken off from the plate ice. The broken cusp radius is calculated by the distance from the contact point and maximum stress point when a plate ice is broken. The icebreaking time is calculated by a time from the ship–ice contact to the ice bending failure. The bending stress in the plate ice σ_b in various ship–ice contact conditions are calculated by using FSI. A database of an icebreaking force, area and time was made. In numerical simulations for different ship–ice contact conditions, the icebreaking force, area, and time at each contact point can be derived from this database.

An alternative mode of ice failure is splitting. A splitting failure occurs because of normal tensile stresses. The splitting force is obtainable as (Michel, 1978 and Cammaert, A.B. et al., 1988)

$$F_s = nLh\sigma_t \tag{4}$$

where σ_t stands for the tensile strength of the ice and n signifies a shape factor for the structure which varies as the wedge angle. L and h respectively denote the length and thickness of ice floe. As described in this paper, the shape factor n is 0.25 (Cammaert, A.B. et al., 1988). The crack of the splitting is assumed to propagate normal to the ship waterline.

Motions Equations and Contact Force

Physically based modeling (Baraff, D., 1997) is applied to calculate the ice floe and ship motions. Ship and ice floe are assumed to be a rigid body. A circle contact detection is applied for ship–ice and ice–ice contacts as described above section. The motions of ship and ice floe are described by 3DOF rigid body equations. The position and orientation of ice floe are solved by Newton's second law. A collision response between two objects (ship–ice and ice–ice) is calculated using an instantaneous impulse. The impulse vector **J** in a normal direction at the contact surface can be written as;

$$\mathbf{J} = j \cdot \mathbf{n}_{ik} \text{ where, } \quad j = \frac{-(1+\varepsilon)v_{ref}}{\frac{1}{m_i} + \frac{1}{m_k} + \mathbf{n}_{ik}\left\{\left(\mathbf{I}_i^{-1}(\mathbf{r}_i \times \mathbf{n}_{ik}) \times \mathbf{r}_k\right) + \left(\mathbf{I}_k^{-1}(\mathbf{r}_k \times \mathbf{n}_{ik}) \times \mathbf{r}_i\right)\right\}}. \tag{5}$$

Therein, j signifies the magnitude of an impulse, $\mathbf{n}_{ik}$ denotes the direction of impulse force of object i received from the object k, ε is a coefficient of restitution, v_{ref} stands for the relative velocity between two objects, m_i represents mass of an object i, and $\mathbf{I}_i$ is the inertia of an object i. Also, r_i is the displacement vector representing the displacement from a center of mass of object i to the center of the contact circle. The mechanical friction force of the Coulomb model described by Eq. (3) is presented in the direction of horizontal to a surface of contact. In the numerical simulation, the time interval of an impulsive response is assumed to be 0.5 s, which is used to transfer from impulsive force [N·s] to peak force [N].A fluid force of surrounding water acting on an ice floe is represented as:

$$\mathbf{F}_w = -\mathrm{C_D} A \frac{1}{2} \rho |\mathbf{v}| \mathbf{v} \quad (6)$$

where C_D signifies the drag coefficient, A denotes a projected area, ρ represents water density, and **v** stands for the ice floe velocity. The fluid force is opposite to the ice floe velocity. In the numerical simulation, the drag coefficient C_D is 0.5. A buoyancy force at the gravity center of the ice floe is considered. For simplicity, other fluid forces related to the ship motion are neglected.

Ice Removal and Ice Breaking

During ship–ice interaction, the ice floe size is major variable for icebreaking scenario. When a ship collide with ice floe, a small ice floe is simply removed. Splitting and bending failure occur in a large-sized ice floe. As described in this paper, it is simply determined that the direct rotation of a small ice floe is occurred when an ice floe size L is smaller than a characteristic length of ice l (Lu et al., 2016). A characteristic length of ice is represented as:

$$l = \sqrt{Ehi^3 / 12(1-\nu^2)/(\rho_w g)} \quad (7)$$

where, E signifies Young's modulus of an ice, h_i denotes the plate ice thickness, ν represent Poisson's ratio ρ_w, stands water density, g is gravitational acceleration. In the larger ice floes than the characteristic length of ice, splitting occurs when an impulse between the ship and ice floe calculated using Eq. (5) is larger than a splitting force obtained by Eq. (4). Bending failure occurs in all remaining ship–ice contacts when a collision force is less than splitting force. An ice floe alternates with ice breaking (bending or splitting) and ice removal (motion of ridged body) within the time interval Δt. During the ice removal contact, ice crushing occurs when the impulse calculated using Eq. (5) is larger than ice-ice contact force calculated using Eq. (1).

RESULTS AND DISCUSSIONS

Numerical Model

Numerical simulations that calculate repetitive ice breaking and ice removal of pack ice have been conducted. The icebreaker waterline and the pack ice model for simulations are shown in Figure 3. A virtual icebreaker (Length × Breadth = 120×24 m) is modeled. The water entry angle and bow angle of the model ship are, respectively, 27° and 30°. The displacement and moment of inertia of the icebreaker are, respectively, 10000 t and 5×10^9 kgm^2. Three different sizes of squared ice floes are arranged within 550×300 m area of the pack ice model. In Figure 3, the sizes of ice floes are, respectively, 15×15 m (110 floes), 40×40 m (21 floes), and 110×200 m (2 floes). Free boundary conditions are given in the numerical domain. The ice floes are 0.5 m thick. Young's modulus of the plate ice, E, is 5.4 GPa. The flexural strength of the ice, σ_f, is 1.0 MPa. The compressive strength of the ice, σ_c, is 2.8 MPa. The tensile strength of the ice, σ_t, is 0.8 MPa. The friction coefficients μ between the ship–ice and ice–ice are 0.2. The coefficient of a restitution ε between the ship–ice and ice–ice are 0.1. The density of ice and water are, respectively, 900 kg/m^3 and 1000 kg/m^3. The ship and ice floe motions are described by 3DOF rigid body equations. The radius contact circle that is used to detect the collision points between the ship and ice is 1.0 m. The simulation time step Δt is 0.005 s.

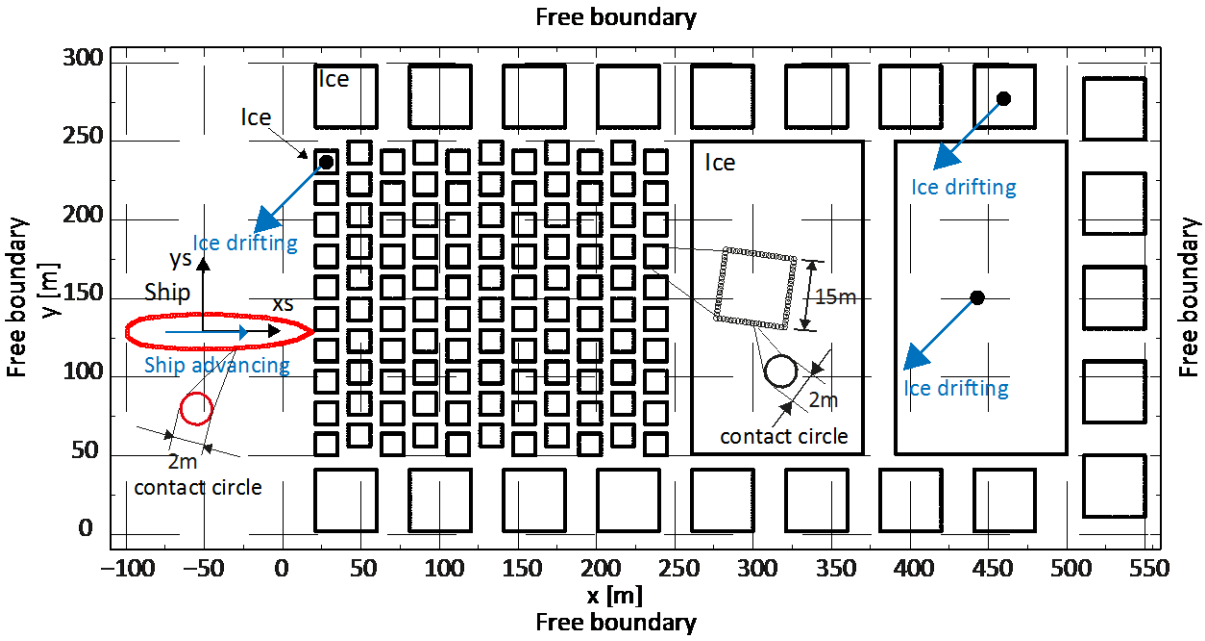

Figure 3. Numerical model when icebreaker advances into ice–covered water with pack ice (The sizes of smallest ice floes = 15×15 m, the number of smallest ice floe = 110 floes).

Effect of Ship Motion and Ice Floe Drifting

Figure 4 presents distributions of ice floes (ice channels) when an icebreaker advances in pack ice. In Figure 4(a), the icebreaker advances with constant ship speed: v_s = 1.0 m/s. In Figure 4(b), the icebreaker advances with constant thrust: $F_t = 0.2\times10^5$ N. In Figure 4(c), the icebreaker advances with constant thrust, and the pack ice floes move with constant drift speed: v_i = 0.071 m/s (v_{ix} = -0.05 m/s and v_{iy} = -0.05 m/s), in which all of the ice floes are drifting in the directions from the portside of icebreaker. The icebreaker removes small ice floes, and makes an ice channel behind the ship. The large ice floe (plate ice) is broken by the bending failures and drifted by the repetitive ship–ice contacts. The ice splitting takes place when the ship–ice collision force acquires the ice splitting force described by Eq. 4. The plate ices divided into 2 or 3 pieces are drifted and removed by ship-ice collision force and icebreaker's advancing. In the comparison with Figure 4 (a), (b) and (c), the ice removals when the icebreaker advances into the small ice floes with different ship–ice conditions show the similar ice channel. On the other hand, the icebreaking by the icebreaker advancing into the large ice (plate ice) show different ice channels. In Figure 4(c), the ship course is changed by the effect of the ice floes drifting from the portside of the icebreaker.

Figure 5 shows the time histories of the peak ice force acting on the icebreaker. The *x*-force represents surge force in ship coordinate system. The *y*-force represents sway force. The ice collision force when the icebreaker collides with small ice floes is smaller than the ice breaking force when the icebreaker collides with a large ice and breaks the plate ice by bending failure. The icebreaking force when an icebreaker advances with constant ship thrust (Figure 5(b) and 5(c)) becomes larger than those with the constant ship speed (Figure 5(a)). Two splitting failure are observed in all of ship–ice interactions in Figures 5(a), (b) and (c). After the second ice splitting, the time history of ice force become more complicated. When an icebreaker advances

with the constant ship thrust and ice drifting speed (Figure 5(c)), the ice force induced by both ice breaking and ice contact are observed. These results show that ship motion and ice drifting have large influence on the icebreaking of a large ice floe (plate ice), but small influence on the ice removal of small ice floes.

Effect of Ice Floes Size

Figure 6 shows the ice floes distribution in different ice floe size. The size of smallest ice floes (15×15 m, 110 floes) in Figure 3 are changed. In Figure 6(a), the size of ice floes are 10×10 m and the number of ice floes are 225 ices. In Figure 6(b), the size and the number of ice floes are, respectively, 20×20 m and 64 ices. In Figure 3, the ice concentration in which smallest ice floes are distributed is 53%, and in both of Figure 6(a) and (b) are 55 %. In Figure 6, the icebreaker advances with constant thrust: $F_t = 0.2\times10^5$ N. The pack ice drift with constant speed: $v_i = 0.071$ m/s. The ice channel width becomes wider depending on the ice floe size. The ship route of icebreaker removes small ice floes is changed by the effect of the ice floe size.

Figure 7 shows time histories of the peak ice force in different floe size. The peak values of the ice collision force when an icebreaker removes the small ice floes depend on the ice floe size. The peak value of the ice removal force colliding with the small ice floes (Figure 7(a)) is smaller than those with large ice floes (Figure 7(b)). The peak value of the ice breaking forces when an icebreaker breaks the plate ice are almost same in Figure 7(a) and (b). In Figure 7(a), the ice breaking starts at 231 s, and ice splitting occurs at 231 s and 366 s. In Figure 7 (b), the ice breaking starts at 293 s, and the ice splitting occurs at 367 s and 454 s. The delay of the

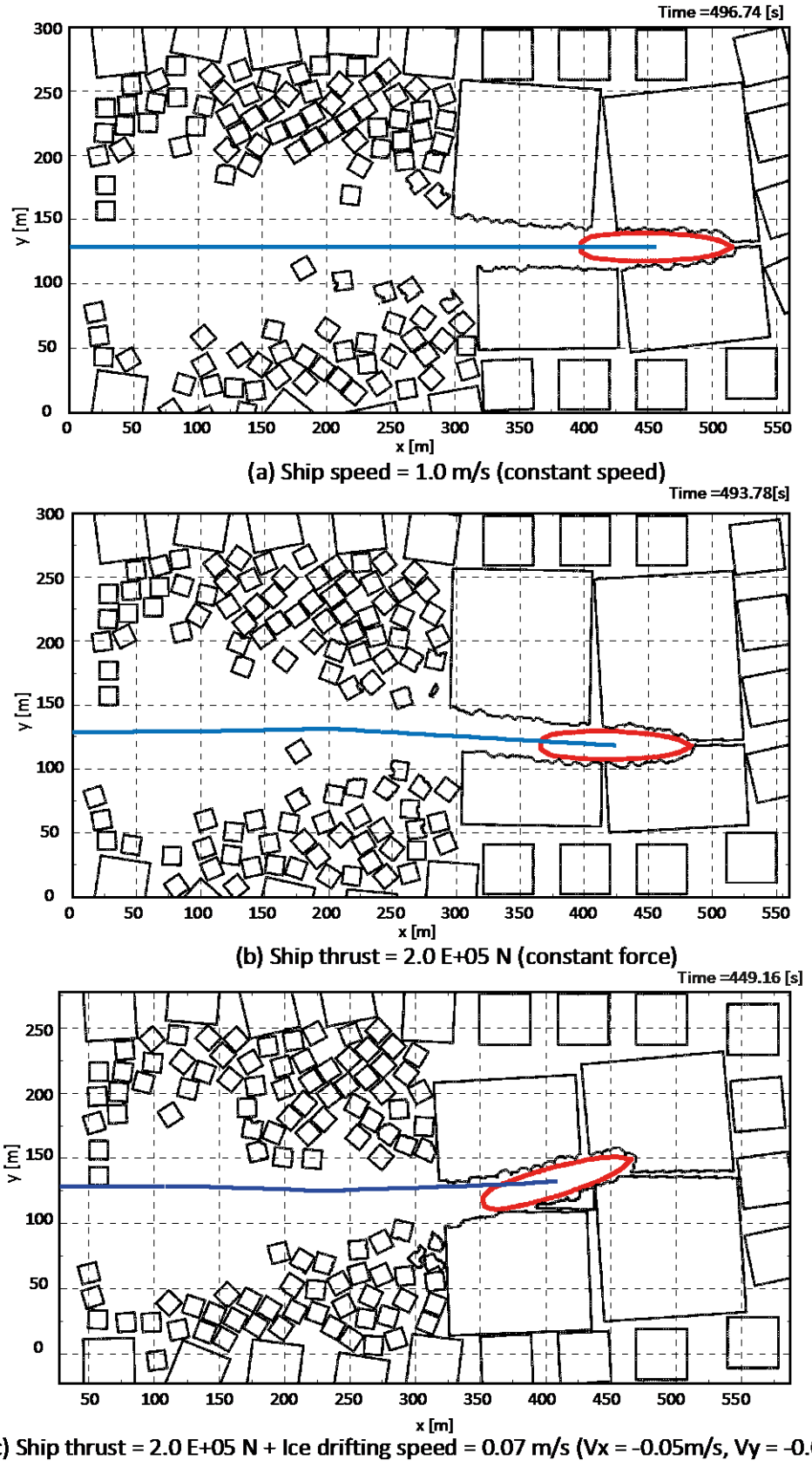

Figure 4. Distributions of ice floes (ice channels) (The sizes of smallest ice floes = 15×15 m, the number of smallest ice floe = 110 floes).

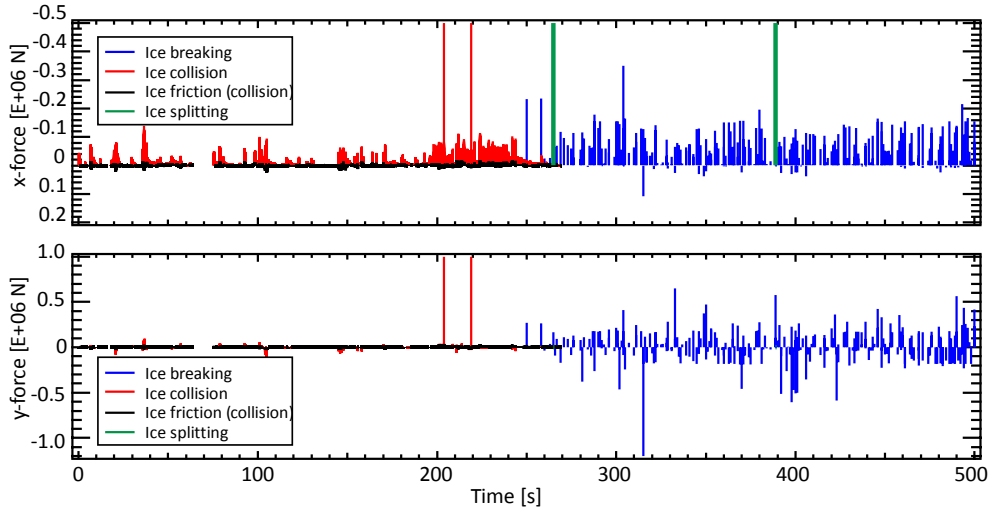

(a) Ship speed = 1.0 m/s (constant speed)

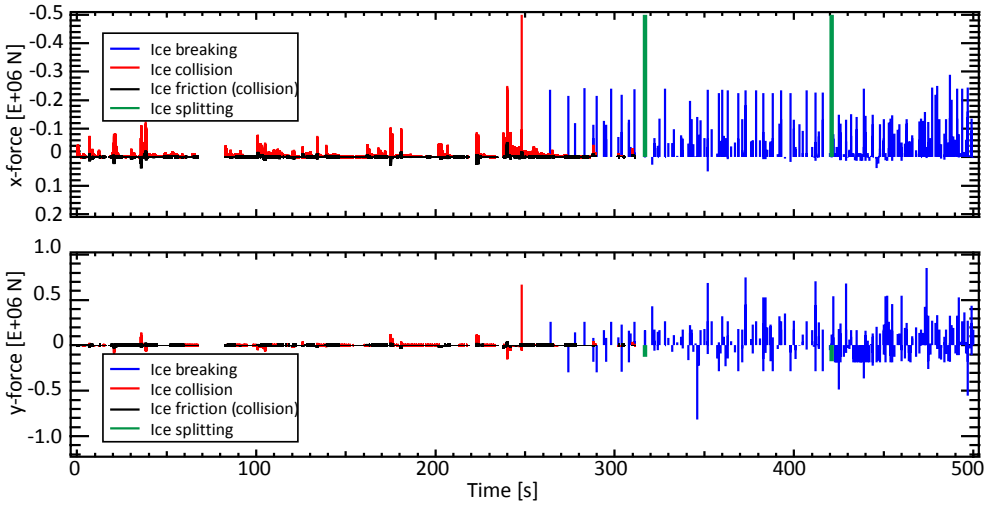

(b) Ship thrust = 2.0 E+05 N (constant force)

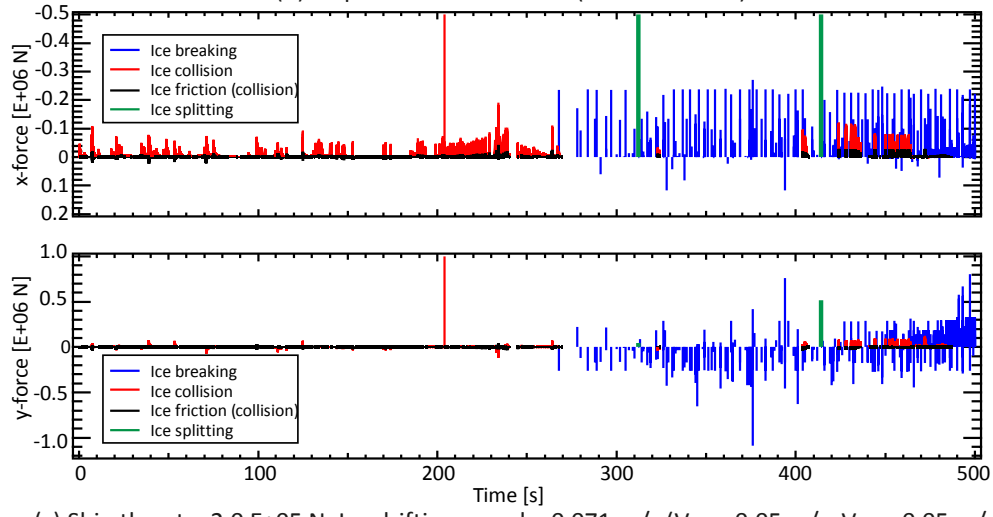

(c) Ship thrust = 2.0 E+05 N, Ice drifting speed = 0.071 m/s (Vx = -0.05 m/s, Vy = -0.05 m/s)

Figure 5. Time history of peak ice force (The sizes of smallest ice floes = 15×15 m).

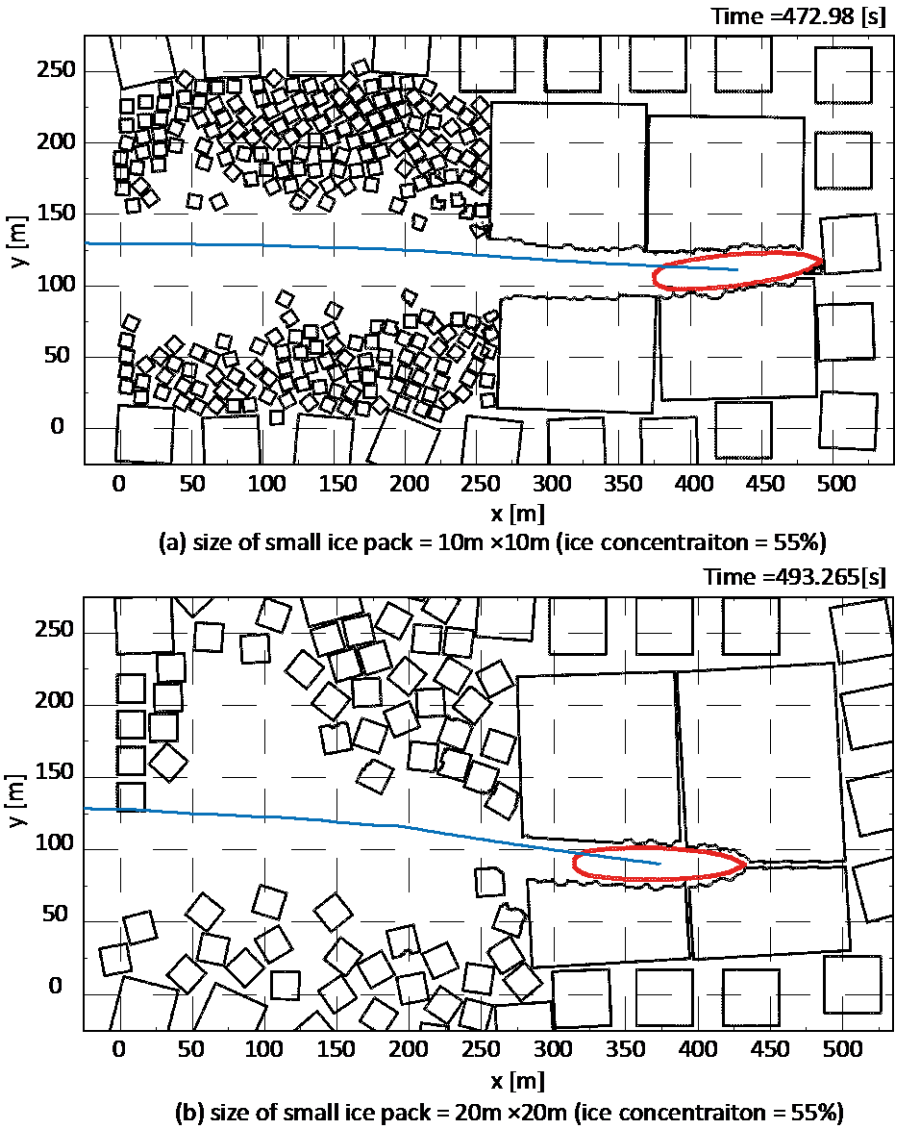

Figure 6. Comparison of ice channel in different ice floes size (The sizes of smallest ice floes = (a) 10×10 m and (b) 20×20 m).

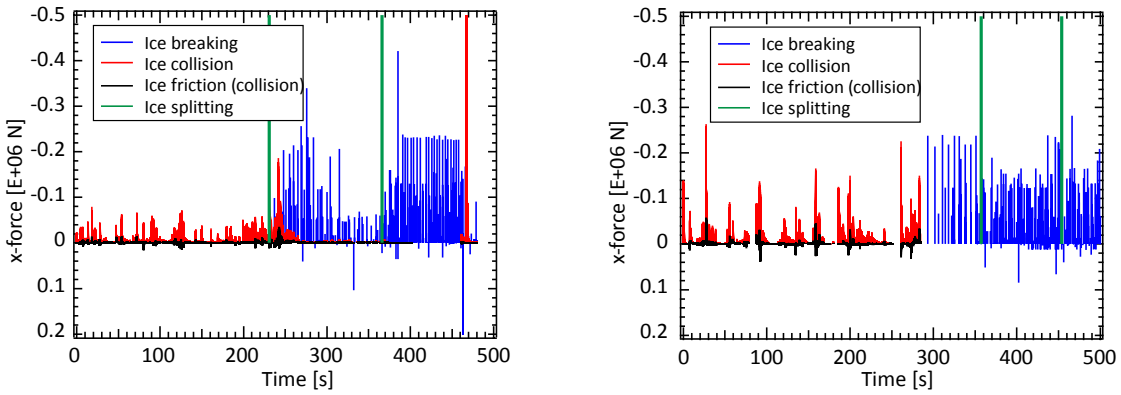

(a) size of small ice pack = 10m ×10m (ice concentraiton = 55%)

(b) size of small ice pack = 20m ×20m (ice concentraiton = 55%)

Figure 7. Comparison of peak ice force in different ice floes size (The sizes of smallest ice floes = (a) 10×10 m and (b) 20×20 m).

icebreaking and splitting can be explained by the speed reduction due to the large contact force when an icebreaker removes the large ice floes. These results show that the ice floe size removed by icebreaker has large influence on both ice breaking of a plate ice and the ship–ice contacts of small ice floe.

CONCLUSIONS

This paper presents a numerical model to calculate ice breaking and ice removal when an icebreaker advances into ice-covered water with pack ice. The ice removal and ice crushing are considered when a small ice collides with a ship or ice floe. The bending failure and splitting are introduced as an ice failure mode of the plate ice. The effect of the ship motion, ice floe drifting and ice floe seize on the ship–ice interaction in pack ice are investigated. The ship motion and ice drifting have large influence on the icebreaking of a plate ice, but small influence on the ice removal of small ice floes. The ice floe size removed by icebreaker has large influence on both ice breaking of a plate ice and the ship–ice contacts of small ice floe. The numerical results show that more realistic numerical modeling including a ship performance and ice conditions is needed for the estimation of managed ice channels. A numerical simulation, however, has the potential to evaluate of ice management strategy. Verification of the numerical model is necessary to identify an efficient mode of shiphandling in actual ice sea.

ACKNOWLEDGEMENTS

This research was supported by JSPS KAKENHI Grant Number 26630455 and 15kk0206. The support from JSPS is greatly appreciated.

REFERENCES

Baraff, D., 1997. Rigid Body Simulation I and II. Siggraph 97, Course notes.

Cammaert, A.B. and Muggeridge, D.B., 1988. Ice Interaction with Offshore Structures, Chapter 7, Static Global Ice Forces on Vertical Structures, Section 7.3, Splitting Mode, pp 232-233.

Dimgliana, J. and O'Sullivan, C., 2000. Graceful degradation of collision handling in physically based animation, *Computer Graphics Forum*, Vol. 19, Issue 3, 239-248.

Farid, F., Scibilia, F., Lubbad, R. and Løset, S., 2014. Sea Ice Management Trials during Oden Arctic Technology Research Cruise 2013 Offshore North East Greenland. *Proceedings of the 22nd IAHR International Symposium on ICE*, pp.518-525.

Hamilton, J., Holub, C.J. and Blunt, J., 2011. Simulation of Ice Management Fleet Operations using Two Decades of Beaufort Sea Ice Drift and Thickness Time Histories. *Proceedings of International Society of Offshore and Polar Engineers*, pp 1100-1107.

Lu, W., Lubbad, R. and Løset, S., 2015a. Tentative Fracture Mechanics of the Parallel Channel Effect during Ice Management. *Proceeding of 23th International Conference on Port and Ocean Engineering under Arctic Conditions*, Paper No.253.

Lu, W., Lubbad, R., Løset, S. and Kashafutdinov, M., 2016. Fracture of an ice floe: Local out-of-plane flexural failures versus global in-plane splitting failure. *Cold Regions Science and Technology*. 123. pp 1-13.

Lubbad, R. and Løset, S., 2011. A numerical model for real-time simulation of ship-ice interaction. Cold Regions Science and Technology. 65(2). pp 111-127.

Michel, B., 1978. Ice Mechanics. Les Presses de I'universite Laval, Quebec.

Sawamura J., Riska K., Moan T., 2008. Finite Element Analysis of Fluid-Ice Interaction during Ice Bending. *19th IAHR International Symposium on Ice,* pp.191-132.

Sawamura J., Riska K., Moan T., 2009. Numerical Simulation of Breaking Pattern in Level Ice at Ship's Bow. *The proceeding of 19th International Offshore and Polar Engineering Conference*, pp.600-607